Nuclear interactions and primary cosmic-ray component around 10^{15} eV viewed through the cluster analysis of γ-ray families

M. Amenomori, E. Konishi, and H. Nanjo
Department of Physics, Hirosaki University, Aomori, Japan

K. Mizutani
Department of Physics, Saitama University, Saitama, Japan

K. Kasahara, S. Torii, and T. Yuda
Institute for Cosmic Ray Research, University of Tokyo, Tokyo, Japan

T. Shirai, N. Tateyama, and T. Taira
Faculty of Engineering, Kanagawa University, Yokohama, Japan

I. Mito
Shibaura Institute of Technology, Tokyo, Japan

M. Shibata
Faculty of Education, Yokohama National University, Yokohama, Japan

H. Sugimoto and K. Taira
Sagami Institute of Technology, Kanagawa, Japan

N. Hotta
Department of Physics, Konan University, Kobe, Japan
(Received 1 December 1981)

An analysis of the γ-ray families ($\sum E_\gamma \gtrsim 100$ TeV) obtained with the Mt. Fuji emulsion chambers was made focusing attention on the cluster structure of families, and the validity of scaling in the fragmentation region in the 10^{15}-eV region was examined by comparing the results with those of artificial families. We deduced that (i) scaling in the fragmentation region (Feynman $x > 0.1$) is not broken appreciably, at least below 10^{15} eV, (ii) scaling in the central region ($x << 0.1$) seems to be broken largely at $E > 10^{15}$ eV; multiplicity increases proportionally to $E^{1/4}$ or even stronger (say, $\propto E^{1/3}$), (iii) the iron component in the primary cosmic rays rapidly increases and occupies 60–70% of the total flux at 10^{15} eV and that of the protons decreases to $\simeq$10%, and (iv) the average transverse momentum of produced pions in the fragmentation region stays within $\sim$400 MeV/c.

I. INTRODUCTION

We have been studying the nuclear interactions at energies exceeding 10^{14} eV through the analysis of atmospheric cosmic-ray spectra and γ-ray families with the Mt. Fuji emulsion chambers.[1] The problem of the primary cosmic-ray spectrum is inevitably involved because of scarce information (especially on the chemical composition) at relevant energies. Because of the steep primary cosmic-ray energy spectrum, the phenomena we observe reflect in general the particle spectra in the very forward region [for the uncorrelated cosmic-ray spectra, the effective Feynman x is $\sim$0.2 where the average number of produced particles is only $\sim$1 (Ref. 2).] However, we may expect that we are able to see the small-x region in some high-energy events produced near the chamber. In fact, we have observed a few events[3] showing very high multiplicity at $x < 0.1$.

Among various models to explain the phenomena, there survive two types at present: (a) one is a

model which assumes scaling[4] and a rapid increase of a very heavy element in the primary cosmic rays, and (b) the other is a model which assumes a scale breakdown in the fragmentation region (shrinkage of the fragmentation region) and high multiplicity with increasing energy for the nuclear interaction and a proton-dominant primary spectrum as in the 10^{12}-eV region. These two alternative approaches seem to be a common trend in understanding air-shower phenomena too (for example, see review papers.[5–7]). The problem is that if model (a) is valid, the high-multiplicity events we have observed are attributed to the breakdown of scaling only in the central region. The test of fragmentation scaling at energies far beyond 10^{12} eV seems possible only through the analysis of cosmic-ray phenomena. (It seems almost impossible to see the particles at $x > 0.1$ by colliding-beam experiments.)

However, both models above are capable of reproducing the experimental data fairly well (say, intensity, lateral spread, energy spectra, and hadron-γ correlation of γ-ray families), so that it is difficult to discriminate the superiority of one model over the other. Let us suppose we have two families with structures as in Fig. 1. The difference is obvious to our eyes but the quantities so far examined would give quite similar values for the two families. We expect that such a difference is a typical one brought about by the models (a) and (b), respectively. A like pattern-recognition problem occurs when we study the families of double- or multiple-core structure in connection with jet or large-transverse-momentum production. We introduce a cluster analysis to resolve these problems.

II. METHOD

A (γ-ray) family[8] is a group of high-energy (say, > 1 TeV) particles generated by a primary cosmic ray. The basic information obtainable for a family is the energy and relative position of each recorded particle. In the target diagram of a family, we usually observe substructures which may be called clusters. To be definite, a cluster in a family is a group of particles having similarity which is expressed by how short the distance between them is. The distance may be defined in various ways. We take[9]

$$\chi_{ij} = (E_i E_j)^{1/2} R_{ij}$$

as the distance between particles (clusters) i and j having energies E_i and E_j. R_{ij} is the geometrical

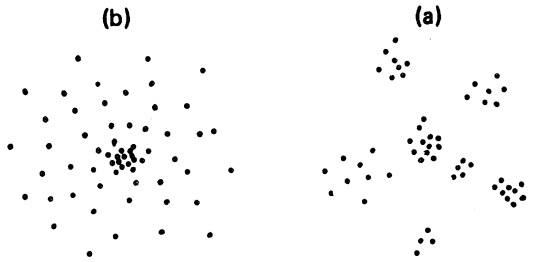

FIG. 1. Typical schematic difference of family patterns. Right is apt to be generated by fragmentation scaling models and left by models assuming a breakdown of fragmentation scaling and high multiplicity.

distance between i and j. χ_{ij} has a physically simple meaning for it is directly connected to the relative transverse momentum times the production height ($p_t H$) of i and j, if they are produced at height H. If H is high, energy dissipation may occur but χ_{ij} is kept nearly constant.

The clustering procedure starts first by regarding all N particles with energy greater than a given E^m as N clusters so that N_c (number of clusters) $=N$ at this stage. Then, the mutual distance χ_{ij} is computed for all combinations of the clusters. The minimum distance among them χ^m is compared with a prefixed χ^C, being the characteristic value of the clusterization. If $\chi^m > \chi^c$, the procedure is terminated. Otherwise, the nearest two clusters are combined to form a new cluster, the center of which determined as the energy-weighted center of the two. The procedure above is repeated until N_c becomes one or $\chi^m > \chi^c$ is reached.

χ^c is set to various values. $\chi^c = 2$ TeV cm would gather cascade particles originated from a single electron or photon (so called decascading[12]), because a cascade particle of energy E spreads roughly within $r \sim$ (radiation length) $\times$ (scattering energy)$/E \simeq$ (500 m) $\times$ (20 MeV)$/E$ so that we may put $\chi^c \sim 2Er \simeq 2$ TeV cm. $\chi^c = 40$ TeV cm may correspond to gathering particles originated from a jet, for if the jet is produced at $H \sim 500$ m above the chamber, jet particles spread mostly within $Er \sim Hp_t \sim$ (500 m) $\times$ (400 MeV) so that we may put $\chi^c \sim 2Er \sim 40$ TeV cm. (Note that χ does not change much if H becomes greater.) However, these are a rough picture on χ^c so that it is rather better to regard it as a conventional parameter.

After the final clusterization is completed, we sometimes discard the clusters with energy less than 10 TeV so that the effect we look for not be masked by low-energy clusters. (Generally, lower-energy clusters are apt to be generated by interac-

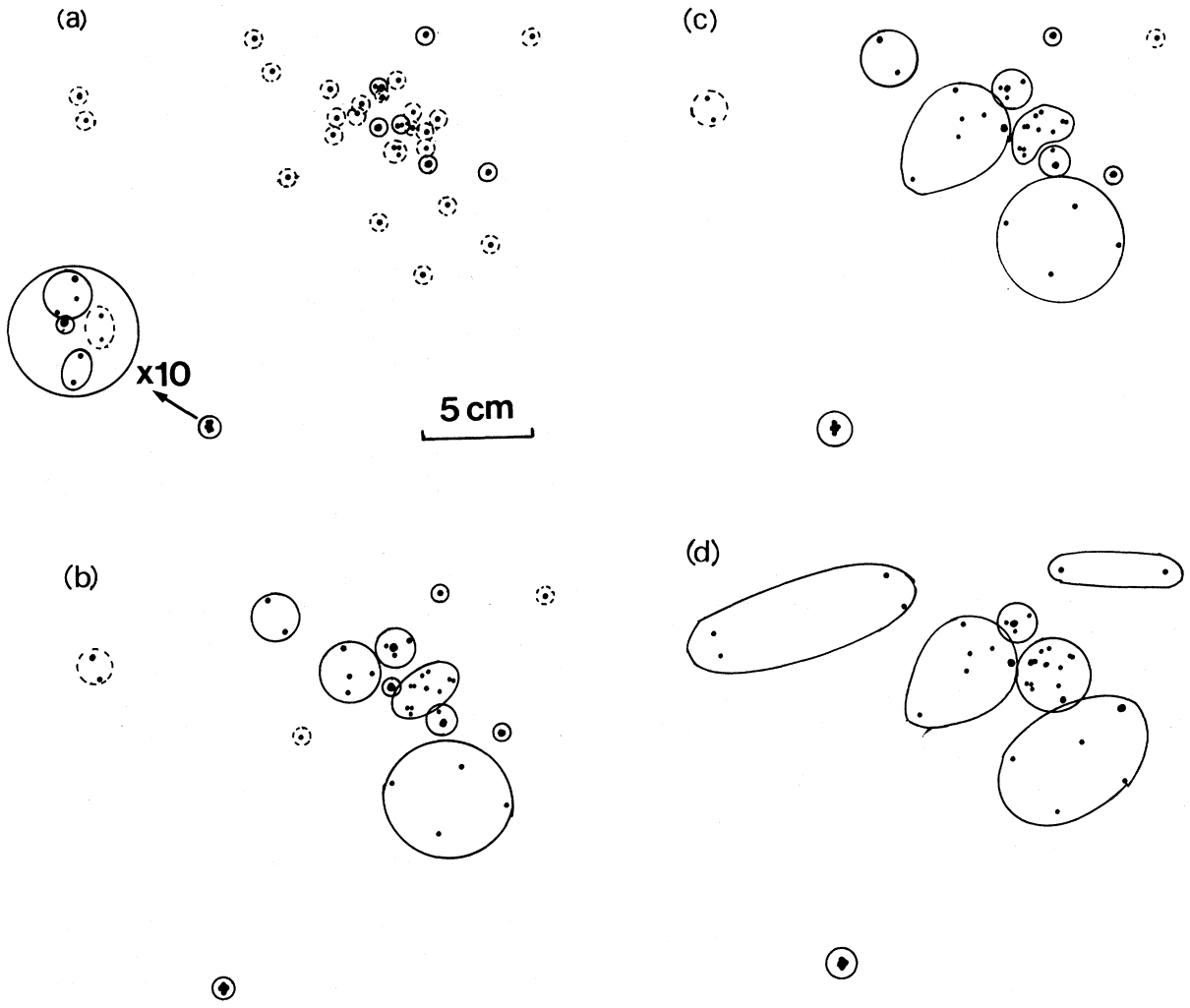

FIG. 2. Example of the clusterization of a family, FE-065. Dotted circle shows a cluster of energy less than 10 TeV, and solid one greater than 10 TeV. The values of χ^c (in TeV cm) are (a) 2, (b) 20, (c) 40, and (d) 80, respectively. The energy of the event is 310 TeV and lower-left cluster of energy 82 TeV consisting of 10 γ rays adds peculiarity to the event.

tions at higher altitudes.)

Figure 2 illustrates the results of the clusterization with various χ^c applied to a family.

The notations we use are illustrated in Fig. 3: N^* is the number of particles in a cluster, N^c the number of clusters in a family. We use $\langle\ \rangle_f$ for the averge in a family and $\langle\ \rangle_c$ for the one in a cluster, e.g., $\langle R_c \rangle_f$ is the average of the cluster spread in a family.

III. NOTES ON THE EXPERIMENTAL DATA AND THE MONTE CARLO SIMULATION

The experimental data used are the families obtained with the Mt. Fuji emulsion chambers. Showers in family are regarded as γ rays, if the starting point of the cascade showers in the chamber are less than 6 cascade units (c.u.) and they show no successive interaction structure; otherwise they are regarded as hadrons. The present results are almost unchanged if we employ 4 c.u. for this criterion. The analysis is made on the γ-ray part.

The minimum unbiased energy of the recorded γ rays is estimated to be $E^m=2$ TeV but sometimes we use $E^m=4$ TeV, too, to be sure of being free from the possible detection loss effect or to compare the result with that by $E^m=2$ TeV. Table I shows the number of families used in the present analysis.

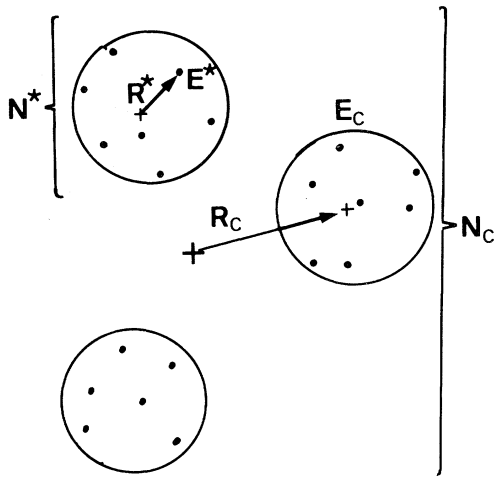

FIG. 3. Illustration of the notations.

We compare the experimental data with the data of a Monte Carlo simulation of which the details are given in Ref. 13. It should be noted that in that calculation no large p_t tail nor explicit jet structure in produced particles are introduced. Also no break of scaling in the central region is assumed in the scaling model. (Its effect will be small in the statistical treatment of families.) The Monte Carlo data have been processed to meet the experimental conditions, among which the finite chamber-block size (usually 40 cm$\times$50 cm unit) effect and γ-hadron mixing (hadron-induced showers observed at shallow depths in the chamber are regarded as γ rays and vice versa) are to be mentioned.

A brief summary of the models in the simulation is listed in Table II. Models are denoted in the symbol column: *P* means the proton primary, *M* the primary of mixed chemical composition, Fe the iron primary, *S* scaling of the production spectrum, *I* the increasing cross section with energy ($\sigma \propto E^{0.06}$), and *F* the fireball model in which the mass increases proportionally to $E^{1/4}$ [substantially equivalent to the CKP (Cocconi, Koester, and Perkins) model][14]; this is a model which breaks scaling in the fragmentation region completely, i.e., the fragmentation region shrinks proportionally to $E^{1/4}$ [see Table IV (b)].

TABLE I. Number of families used in the present analysis (minimum energy is 2 TeV).

$\sum E_\gamma$ (TeV)	100–200	200–500	>500
Number	63	31	7

We call attention to the fact that the mixed chemical composition of the primary cosmic rays (*M*) in the simulation is used to realize the model (a) mentioned in I so that the fraction of the iron component rapidly increases with energy.[15] The case where the primary is composed of protons only is unrealistic, but we can regard it as a proton-dominant-primary case where the spectra of other heavy elements have almost the same slope as that of the protons, because in this case the contribution from the heavy elements is small in the family phenomena (especially on the intensity). However, if there were a need to estimate the effects by the heavy primaries, we made simulations with primaries of α, CNO, etc. In this sense, *PF* and *PFI* is the model (b) stated in I.

We shall mainly use models *MSI* and *PF* for comparison with the experimental data, for they survive up to now as mentioned in I. Although *PS* in the sense of the proton-dominant primary has been rejected,[1] because it gives a too high intensity and too small lateral spread of family etc., we use it to demonstrate the effect of heavy primaries.

IV. RESULTS AND DISCUSSIONS

A. Some quantities reflecting the cluster structure

If the difference of the patterns of families is as in Fig. 1, it will be reflected in χ_{ij}: Fig. 1(a) will give larger $\langle \chi_{ij} \rangle$ than Fig. 1(b). Figure 4 shows the integral χ_{ij} distributions constructed by taking all combinations of i and j ($i>j$) in each family ($\chi^c=40$ TeV cm, $E_c>10$ TeV). The experimental data is slightly higher than the *MSI* model prediction but lower than the Fe*S* model. The *PS* and *PF* models give far smaller values than the experimental value. It is worth mentioning that *PS* gives the almost same χ_{ij} distribution as *PF* in spite of the fact that *PF* gives a lateral spread of γ rays roughly twice as large as *PS*.[1] This indicates that χ_{ij} is sensitive to the cluster structure. Large χ_{ij} by Fe*S* is, however, mainly due to the large lateral spread which is twice that of the *PF* model.[1]

The χ_{ij} distribution by the *PF* model might be improved to meet the experimental data if heavy primaries were introduced, though this generates new contradictions in other points, as will be demonstrated soon. It has been found that the distribution of $\chi_{\max}$ (= maximum of χ_{ij} in each family) or $\langle \chi_{ij} \rangle_f$ shows quite a similar tendency as the χ_{ij} distribution.

TABLE II. Summary of assumptions of the Monte-Carlo calculation.

Primary Type	Primary Slope[a]	Interaction	Symbol[b]
Proton	$2.7 \rightarrow 3.0$	Scaling	*PS,PSI*
		Fireball	*PF,PFI*
Mixed	(p,α)	Scaling	*MSI*
	$2.8 \rightarrow 3.0$		
	(L,M,H,VH)		
	$2.6 \rightarrow 3.0$		
	(Fe)		
	$2.3 \rightarrow 3.0$		
Iron	$2.7 \rightarrow 3.0$	Scaling	Fe*S*

[a] $\beta \rightarrow \gamma$ denotes $E^{-\beta}dE$ at $E < 10^{15}$ eV and $E^{-\gamma}dE$ at $E > 10^{15}$ eV.
[b] *I* is attached if the cross section is made to rise as $\sigma \propto E^{0.06}$.

In Fig. 5 is plotted the dependence of $\langle N_c \rangle_f$ on the value of χ^c ($E_c > 10$ TeV). We see that the *PF* model gives too large $\langle N_c \rangle_f$ as compared to the experimental data and the inclusion of heavy primaries would simply result in enlarging the difference. From the comparison of the two graphs for $\sum E_\gamma = 100-200$ TeV and $\sum E_\gamma = 200-500$ TeV, the *MSI* model seems to suggest a higher Fe ratio in the higher-energy primary and/or a jet production contribution to get a more consistent picture with the experimental data.

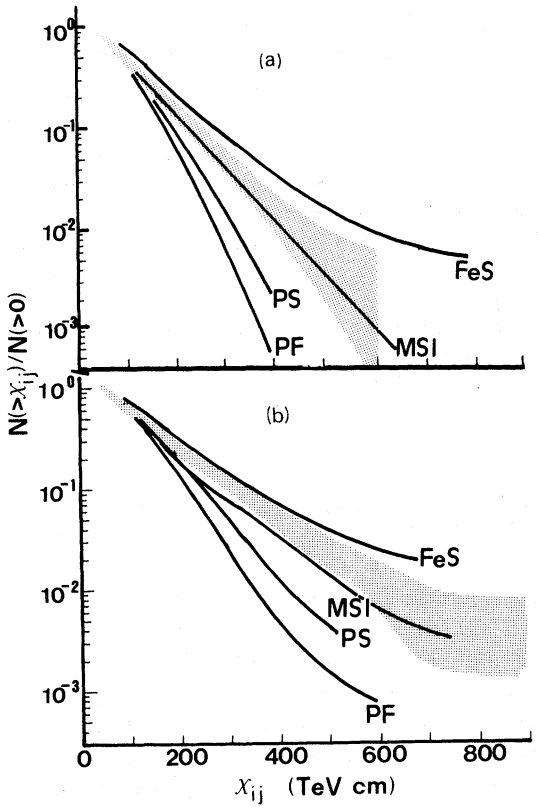

FIG. 4. Normalized integral χ_{ij} distribution superposed for many events. Shadow area shows the experimental data. Width of the shadow represents the statistical error. Monte Carlo calculations are shown by solid lines with symbols to specify the models. (a) $\sum E_\gamma = 100-200$ TeV, (b) $\sum E_\gamma = 200-500$ TeV.

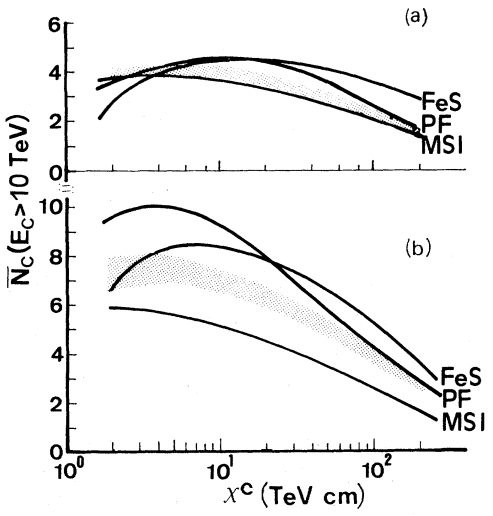

FIG. 5. Dependence of the average number of clusters with energy greater than 10 TeV on the characteristic parameter χ^c. Experimental data is represented by shadow area of which width shows the statistical error. (a) $\sum E_\gamma = 100-200$ TeV, (b) $\sum E_\gamma = 200-500$ TeV.

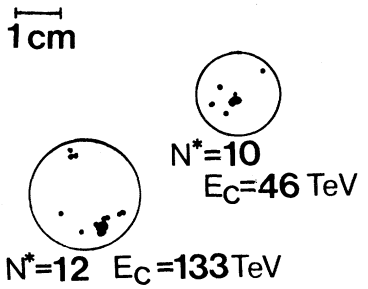

FIG. 6. Example of the double-core families, FB-029. Clusterization is done by $\chi^c=40$ TeV cm. The energy of the event is 196 TeV and consists of 25 γ rays. They are decomposed into two clusters with $\chi_{12}=300$ TeV cm and other small clusters (<10 TeV) far away from the center (small ones are not shown).

B. Double-core family

We sometimes observe double-core families consisting of two well separated groups of γ rays as illustrated in Fig. 6. The chance-coincidence probability that two different families be misidentified as a double-core family may be calculated as the number of families with energy more than the smaller core, falling within the radius of R between the two and relative angle difference $\Delta\theta$. For one-year exposure at a mountain level depth Z, probability is expressed as

$$P\sim 0.13(R/20\text{ cm})^2(\textstyle\sum E_\gamma/10\text{ TeV})^{-1.4}$$
$$\times\frac{Z}{\Lambda}\exp\left[\frac{650-Z}{\Lambda}\right]\exp\left[-\frac{Z\theta^2}{\Lambda}\right]\pi\Delta\theta^2\,,$$

where θ is the zenith angle of the family, Λ the attenuation length of family (~ 110 g/cm^2) and $\sum E_\gamma$ is the energy of the smaller core summed for $E_\gamma>2$ TeV. Putting $R=20$ cm, $\sum E_\gamma=10$ TeV, $Z=650$ g/cm^2, and $\theta\sim 0$, we get $P\sim 2\Delta\theta^2$ so that it is statistically negligible if $\Delta\theta$ is order of 10^{-2}, which is the average relative angle difference for family identification.

It is important to know that their origin is reducible to the large p_t production or a mere fluctuation brought about by the complexity of family phenomena. To identify the double-core families quantitatively, we adopt the following criterion which is similar to those used by the Chacaltaya group[11]: (i) $\sum E_\gamma\gtrsim 100$ TeV ($E_\gamma>E^m$), (ii) $N_c=2$ after clusterization with $\chi^c=40$ TeV cm (clusters of $E_c<10$ TeV are discarded), (iii) $R_{12}>5\times\max(\langle R_1^*\rangle_c,\langle R_2^*\rangle_c)$, and (iv) $E_{c1}+E_{c2}>0.8\sum E_\gamma$.

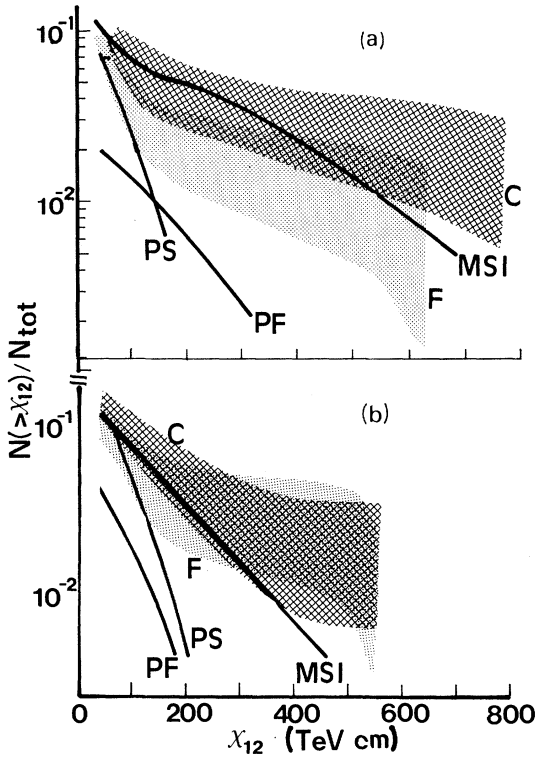

FIG. 7. Integral χ_{12} distribution of the double-core events. Frequency is normalized by the total number of the families. Shadow area with symbol F is our data and that with C is the Chacaltaya data obtained by our algorithm. Width of the shadow shows the statistical error. Results of the Monte Carlo calculations are denoted by solid lines with symbols to specify the models. (Only average values are shown.) (a) $E^m=2$ TeV, (b) $E^m=4$ TeV.

The integral distribution of χ_{12} of the double-core families thus identified is shown in Fig. 7(a) for $E^m=2$ TeV and (b) for $E^m=4$ TeV. The frequency is normalized by the total number of families. The number of double-core families in the experimental data is order of 10%. The *PF* model is not capable of producing double-core families compatible with the experimental one and has been proved not to be improvable by the inclusion of heavy primaries. The *MSI* model gives a fairly good picture comparable to the experimental data. It is understood that families of large χ_{12} by *MSI* are generated by heavy primaries such as α, CNO since *PS* does not yield large χ_{12} and iron primaries never generated double-core families.

The deviation at the largest χ_{12} region for $E^m=4$ TeV might be due to the jet of large p_t, but

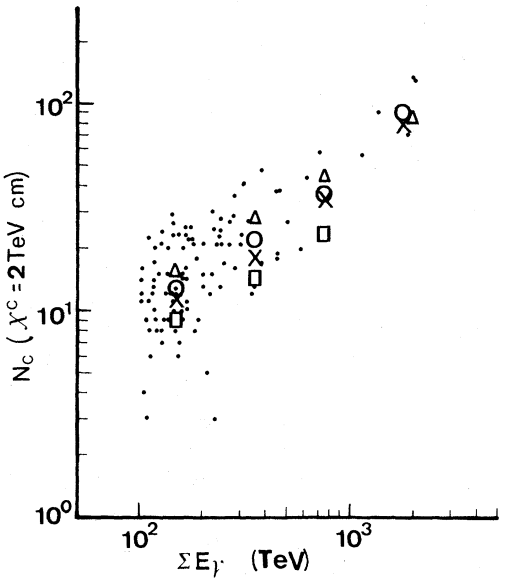

FIG. 8. Correlation of the number of clusters by decascading N_c (χ^c=2 TeV cm) vs. $\sum E_\gamma$. Dots represent Mt. Fuji data of which averages at appropriate $\sum E_\gamma$ intervals are denoted by open circles. The results of the Monte Carlo calculation are shown only by the average: Δ*PF*, $\times$*MSI*, □*PS*.

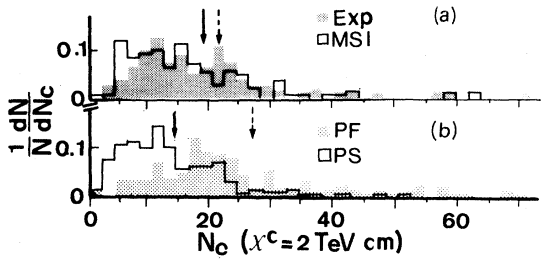

FIG. 9. Distribution of the number of clusters by decascading (χ^c=2 TeV cm). Solid line arrow shows the average position for the histogram by solid line, and broken one for that by shadow. (a) Mt. Fuji data (shadow) and *MSI* model (solid line), (b) *PF* model (shadow) and *PS* model (solid line).

there remains problems of the fraction of the heavy primaries assumed in *MSI* and statistical fluctuation. At any rate, we are just on the border of the large-p_t effect as far as we use χ_{12} defined as such. Further investigation should be made by introducing an explicit jet production cross section in the Monte Carlo calculation.

In the same figure are also shown the Chacaltaya group data,[16] obtained by the same procedure (χ^c=44 TeV cm has been adopted to compensate the height difference). The tendency is quite similar to our data.

C. Problems of high multiplicity, jets, and large p_t

If we take a simple picture that the families we observe are produced, say, 1 km above the chamber and the decascading (χ^c=2 TeV cm) or jet extraction (χ^c=40 TeV cm) procedure is really effective, we may say that N_c (with χ^c=2 TeV cm) and E_cR_c (with χ^c=40 TeV cm) give us direct information about the multiplicity and jet p_t of the nuclear interactions. If successive interactions and dispersive production heights do not distort the picture above seriously, as assumed by some authors,[17,18] the statement above may hold true. However, this should be examined through the comparison with Monte Carlo calculations.

1. *Multiplicity*

A scatter diagram of N_c vs $\sum E_\gamma$ after the decascading procedure is shown in Fig. 8, together with the mean values of N_c at appropriate $\sum E_\gamma$ intervals. One of the advantages of using the decascading procedure is that, when counting the number of showers, the ambiguity due to spatially unresolvable showers can be eliminated. The figure tells us that the increase of N_c with $\sum E_\gamma$ takes place both in *MSI* and *PF*, indicating that the heavy primaries and successive interactions give the effect analogous to the rapid increase of multiplicity as in *PF*. The distribution of N_c itself is shown in Fig. 9 where we see a wide spread of the experimental data.

In Figs. 8 and 9 we observe that *MSI* gives a fairly good agreement with the experimental data although more heavy primaries and/or high-multiplicity effect seem to be needed. The *PF* model gives larger values than the data and inclusion of heavy primaries would enlarge the deviation.

As stated earlier, the family phenomena are relatively insensitive to the central region ($x < 0.1$), if fragmentation scaling holds, so that the statistical analysis here presented tells that no remarkable shrinkage of the fragmentation region should occur rather than multiplicity itself.

For multiplicity we must seek further information. As mentioned in I, we have observed a few events which are most naturally interpreted to be large-multiplicity events without particles in the

fragmentation region. Especially one event named F4-589 shows clear evidence that 150–200 π^0's (or rather 300–400 γ's)[19] are produced by one nuclear interaction occurred at $\sim$200 m above the chamber. The incoming nucleon energy is estimated to be $\gtrsim$4000 TeV. The highest γ-ray energy contained therein is $\sim$60 TeV so that almost no particle is produced at $x > 0.01$. The total multplicity of the event may reach $\sim$500, which is far larger than $\sim$200, being the average multiplicity extrapolated by the $E^{1/4}$ dependence from 1 TeV to 10^4 TeV. Other less-clear events show a similar tendency. The problem is, as mentioned earlier, that these high-multiplicity events are attributed to CKP-type interactions or scale breaking in the central region only.

On the other hand, we have the following information: an accelerator experiment by 400-GeV protons,[20] balloon experiments[20,21] ($E_0 \sim 10$ TeV), and the Chacaltaya C-jet experiment[11] ($E_0 \sim 100$ TeV)[11] seem to show fragmentation scaling while the pseudorapidity density at $x << 0.1$ clearly increases with incoming energy.[22] Its energy dependence is, if we use the power form, approximated by $E_0^{0.1}$.

Our present analysis shows that no appreciable shrinkage of the fragmentation region should occur at least $E_0 < 10^{15}$ eV. Further we have events in the $\sum E_\gamma \sim 1000$ TeV region which are hardly attributable to the CKP-type interactions. These indicate that the scale breakdown in the central region continues to the 10^{16} eV region while the shrinkage of the fragmentation region is not so rapid as the CKP type even above 10^{15} eV and our high-multiplicity events are nothing but a large heap of particles at $x << 0.1$ due to the scale breaking in the central region. Because the high multiplicity events show a very similar tendency, we may regard that the events show more or less the average characteristics of the central region of those events which are not associated with the fragmentation particles. Then the energy dependence of overall average multiplicity above 10^{15} eV would be $\sim E^{1/3}$ or at least stronger than $E^{1/4}$.[23] The large scale breaking in the central region would affect the N_c distribution so that the *MSI* model would get a better agreement with the data with heavy primaries not so much different from the original assumption. (As one may observe that a mixture of *MSI* and *PF* would give a good agreement in Fig. 9.)

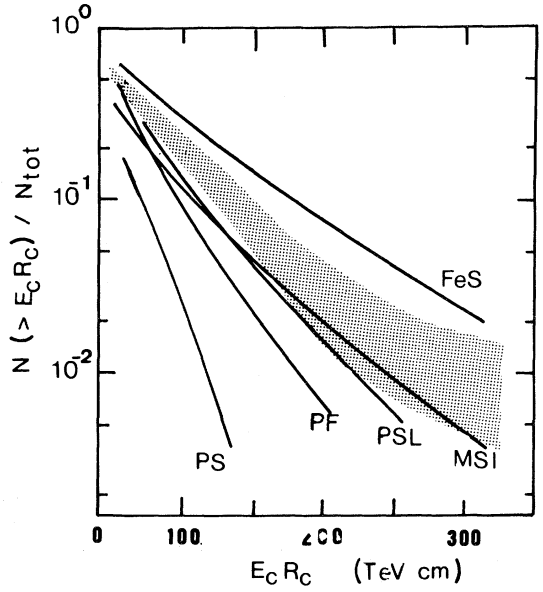

FIG. 10. Integral cluster *ER* distribution normalized by the total number of families. $\chi^c = 40$ TeV cm is used. Mt Fuji data is shown by shadow area of which width stands for the statistical error. The average value of each Monte Carlo calculation is denoted by solid line with symbol specifying the model.

2. p_t and jets

In Sec. B, we examined double-core families in connection with p_t and jet. N_c and E_cR_c with $\chi^c = 40$ TeV cm are also related to the same problem. The integral distributions, normalized to one event, of E_cR_c with $\chi^c = 40$ TeV cm are shown in Fig. 10 ($E^m = 4$ TeV). The experimental data again lies between *MSI* and FeS. The *PS* model never generates large E_cR_c compatible with the experimental data while *PSL* (same as *PS* except $\langle p_t \rangle$ is twice as large as *PS* case) yields a distribution close to the experiment so that p_t is certainly reflected in this distribution. High multiplicity as in *PF* is also a source of large E_cR_c; a small amount of heavy primaries would improve the distribution to meet the experiment without demanding the increase of p_t. However, *MSI*, if its iron abundance is adjusted and the large scale breaking in the central region is incorporated, would give a more consistent picture with the data. Also as in the cases of χ_{ij} and double-core events, a small increase of $\langle p_t \rangle$ or large-p_t jet contribution is a desirable tendency but not necessarily indispensable. In other words, we are just on the border of the large-p_t effect in this distribution too. The transverse momentum discussed here is that of

secondary particles in a very forward region. However, the high-multiplicity events we have show no sign of remarkable increase of the average transverse momentum at $x < 0.1$.[3] The distribution of the number of clusters, $N_c(\chi^c = 40$ TeV cm), or its dependence on $\sum E_\gamma$ is well explained as in the decascading case.

D. Dissection of the Monte Carlo families

Since the Monte Carlo family data provide us the history of the propagation of particles in the atmosphere, we are able to know parameters such as the energy and type of the primary as well as the origin of particular observed particles. We shall illustrate some of the dissection of the artificial families.

The correlation of N_c and $\langle R_c \rangle_f$, parametalized by the type of the primary particles (*MSI* model), is shown in Fig. 11 where we see that heavier primaries have a tendency of giving larger N_c and $\langle R_c \rangle_f$.

Figure 12 shows an example of triple-core families. The event is produced by a proton primary of $E_0 = 4950$ TeV. It is seen that each core is composed of almost one generation. The clusterization

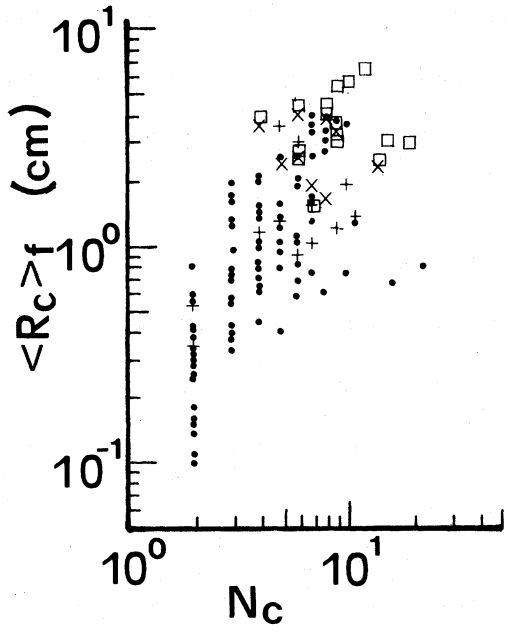

FIG. 11. A sample of the Monte Carlo family dissection. Correlation of $\langle R_c \rangle_f$ vs N_c (with $\chi^c = 40$ TeV cm) of *MSI* model. Points are parametrized by the type of primary cosmic ray: ● proton, + α particles, × *M* and *H*, □ *VH* and Fe.

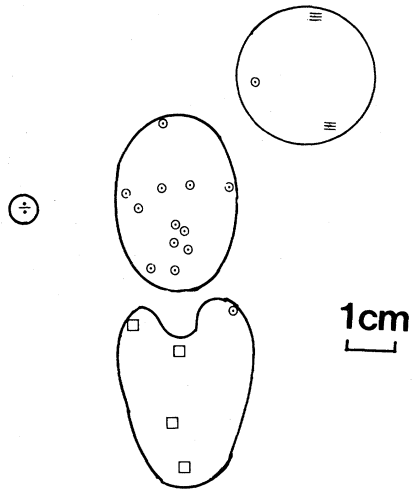

FIG. 12. A sample of the Monte Carlo family dissection. A family generated by a proton primary of $E_0 = 4950$ TeV is clusterized by $\chi^c = 40$ TeV cm to obtain three cores, each of which is composed of γ rays of almost one generation: ≡ denotes γ rays from the atmospheric depth $Z = 320$ g/cm^2, ⊙ those from $Z = 205$ g/cm^2, and □ those from $Z = 600$ g/cm^2.

by $\chi^c = 40$ TeV cm is useful for identifying showers of different generations with ~70% certainty. Separated cores by a proton primary are usually originated from particles of different generations, which have very high energies at production points and penetrate into deep depths. They are a few number of (or single) pions or γ rays.

E. Expected primary cosmic-ray spectrum

As has been shown, the *MSI* model gives a fairly consistent picture with the experimental data. The deviations of its prediction from the experimental data are not serious ones and would be overcome by adjusting the *p*/Fe ratio in the primary and by the large break of scaling in the central region. We shall estimate plausible primaries around 10^{15} eV within this regime. The basic points to be noted are as follows.

(1) All quantities by the present cluster analysis seem to favor a smaller *p*/Fe ratio than originally assumed in the *MSI* model. This is, however, not so large an extent because of the large scale breaking in the central region.

(2) Uncorrelated γ-ray energy spectrum ranging from 1 to 100 TeV at Mt. Fuji shows, on the average, a steep power spectrum with slope ~2.0 and

seems much steeper over 30 TeV.[24] The γ-ray of energy 1TeV corresponds to a primary proton of ~ 30 TeV (for primary of slope 2) to ~ 150 TeV (for slope 1.7), if scaling holds.[25]

(3) The results of the *MSI* calculation tells us that the effect of heavy primaries is well approximated by the simple superposition (at least for energetical aspect of families).[26] The equivalent-proton spectrum obtained by the simple superposition should be consistent with the flux of the uncorrelated γ-ray spectrum and the γ-family intensity.

(4) The spectrum of each primary component should be connected to the measured values at 10^{12} eV, for which we refer to a summary by Juliusson.[27]

The result is presented in Figs. 13 and 14 where the intensity is expressed in (total energy)^2 $\times$(integral flux). (See also Table III.) The proton-spectrum slope should steepen from ~ 1.7 to ~ 2.0 at $\sim 4\times 10^{13}$ eV. On the other hand, the iron-spectrum slope keeps ~ 1.4 up to $\sim 10^{15}$ eV and steepens to ~ 2.0. Hence it surpasses other components already at $\sim 4\times 10^{13}$ eV. This is of course not a measured data but is one model of plausible primaries (say, one may choose somewhat different abundances of α and $M+H+VH$ than presented). Therefore, it is not appropriate to give error bars.

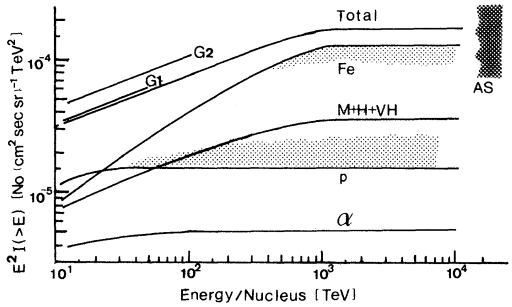

FIG. 13. Expected primary cosmic-ray spectrum in integral form. Intensity is multiplied by E^2. Energy is expressed in total nucleus energy. Fe denotes the iron component, $M+H+VH$ the sum of the components of charge between 6 and 24, p the protons, and α the α particles. G1 and G2 are the results by Grigorov *et al.*[28,29] for total flux. Shadows attached to Fe and p components indicate that the solid lines are an upper (for Fe) and lower (for p) estimation. Width of the shadows may be taken as roughly representing permissible levels in our estimation. Shadow with symbol AS is an extrapolation of majority of air-shower results to the lower-energy region.

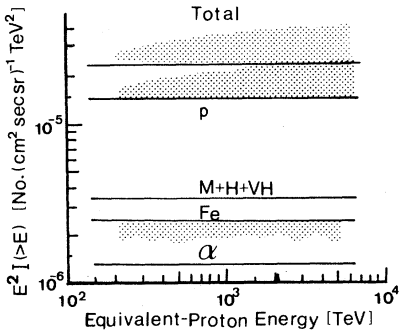

FIG. 14. Equivalent-proton spectra of various components obtained from Fig. 13 by the simple superposition procedure. Notations are the same as in Fig. 13. This represents the relative importance of each component in observed family.

The basic uncertainty of the estimation comes from the degree of the rising cross section, possible change of the leading-particle spectrum (i.e., change of the inelasticity to higher values), and possible small shrinkage of the inclusive spectrum in the fragmentation region, presumably connected with the large scale breaking in the central region. In view of these factors, one should regard that the iron spectrum presented in Fig. 13 is an upper bound estimation and that of protons is a lower bound one. These are indicated by shadows in the figure.

It is worth mentioning that completely different experimental procedures have arrived at quite similar conclusions about the primary composition around 10^{15} eV.[30,31]

V. CONCLUSIONS AND REMARKS

From the present analysis, we deduce the following conclusions

(1) Scaling in the fragmentation region ($x > 0.1$) is not broken appreciably at least at $E < 10^{15}$ eV.

(2) Scaling in the central region ($x << 0.1$) is broken largely at $E > 10^{15}$ eV. This break seems to continue from a few hundred GeV to the 10^{16} eV region. The degree of break seems to become stronger at $E > 10^{15}$ eV; multiplicity is expected to be proportional to $E^{1/4}$ or even stronger (say, $E^{1/3}$) at $E > 10^{15}$ eV.

(3) The fraction of the iron component in the primary cosmic-ray spectrum increases rapidly as energy goes higher and that of protons becomes smaller. The ratio of the iron component to the total primary flux is 60—70% and that of protons

TABLE III. Fraction of various components in the expected primary cosmic rays at two primary energies (in percent). Light-group nuclei are neglected. Values for M, H, and VH are a plausible composition.

Energy (eV) Component	10^{14}	10^{15}
p	20	9
α	6	3
M	8	5
H	26 { 13	20 { 10
VH	5	5
Fe	48	68

$\sim 10\%$ at 10^{15} eV. Other heavy primaries (20—30%) are also needed. A plausible model of the primary is shown in Fig. 13.

(4) The average transverse momentum of pions in the fragmentation region at interactions of $\sim 10^{15}$ eV is not so much different from the usual values (at most ~ 400 MeV/c).

A schematic illustration of the change of the particle spectrum in hadron collisions is given in Table IV. Our analysis shows that (a) is valid and (b) is very unlikely.

We wish to add the following remarks on each of the conclusions above.

(i) Shrinkage of the fragmentation region as in the CKP model is too rapid (shrink rate is proportional to $E^{1/4}$), but we cannot exclude a small degree of shrinkage (say, $E^{0.05}$). Rather we anticipate such small breakdown because the large break of scaling in the central region presumably affects the fragmentation region. The shrinkage may become stronger at $E > 10^{15}$ eV, because the families of $\sum E_\gamma > 1000$ TeV we observed seem to favor the CKP-type interpretation.[3] This is an open question at present.

(ii) We expect that the collisions giving fragmentation particles ($x > 0.1$) are not associated with the large heap of particles at $x \ll 0.1$ and vice versa. (The same tendency has been observed in the accelerator energy region.) Collisions giving a large number of particles only in the central region are observed as high-multiplicity events in some case. As mentioned in (1), the cross section of the collisions giving fragmentation particles may become smaller at $E > 10^{15}$ eV, as if the interactions in this region look close to the CKP type.

(iii) A probable small degree of shrinkage of the fragmentation region, as mentioned in (i), affect the estimation so that these values should be taken as an upper (for Fe) and a lower (for p) one, although we expect the effect is not so large.

(iv) This is true even if large scale breaking in the fragmentation region exists (as in the CKP model). Although the average transverse momentum is kept almost constant, some of the events we have observed clearly show a large transverse momentum (say, the event TITAN[32]).

Other remarks are as follows: We discarded the CKP-type rapid scale breaking in the fragmenta-

TABLE IV. Schematic illustration of the change of nuclear interaction. (a) is expected and (b) is very unlikely. y is the rapidity normalized by that of the projectile. $y = 0$ corresponds to $x \simeq 0.15$.

	$\frac{1}{\sigma} x \frac{d\sigma}{dx}$	$\frac{1}{\sigma} \frac{d\sigma}{dy}$	Remark
(a)	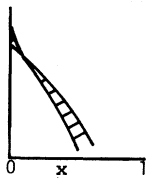	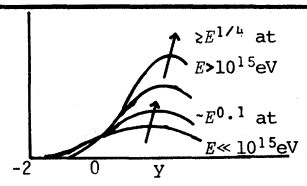	Primary is iron dominant. Small shrinkage of x distribution may exist.
(b)	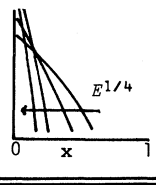	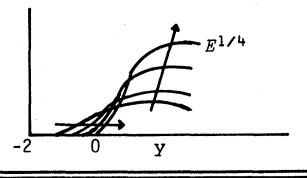	Primary is dominated by protons.

tion region. However, if such a model should be resumed we must introduce the following modifications; (i) shrinkage should be appreciable only above 10^{13} eV, and (ii) a strong jet structure or anisotropy in produced particles must exist. However, it would be difficult to think of such mechanisms in the CKP-type high-multiplicity models.

We have seen that the primary-particle type plays an essential role in the family pattern formation. If we could know the primary particle type to be a proton, we would be able to get reliable information on the nuclear-interaction characteristics at ultra-high energies. The simultaneous observation of γ families and electron-air-shower size is a very promising way for extracting families generated by proton primaries.[33]

ACKNOWLEDGMENTS

The authors would like to express their gratitude to Sengen Shrine, Kawaguchiko office of The Agency of Environment Maintenance, and Gotenba Meteorological Observation Station for extending every facility necessary for carrying out the experiment at Mt. Fuji. They are also indebted to the technical staff of the Institute for Cosmic Ray Research, University of Tokyo, Mmes. E. Mikumo, K. Sato, M. Tsujikawa, S. Toyoda and Mr. T. Kobaysahi, and to Miss Y. Sato of Hirosaki University for the scanning of events or their cooperative efforts. The data analysis was done using the computer FACOM M180II AD of Institute for Nuclear Study, University of Tokyo.

[1]Mt. Fuji collaboration, M. Akashi *et al.*, Phys. Rev. D 24, 2353 (1981). A part of the present analysis has been included therein.

[2]For example, K. Kasahara and Y. Takahashi, Prog. Theor. Phys. 55, 1896 (1976).

[3]M. Akashi *et al.*, in *Proceedings of the Fourteenth International Conference on Cosmic Rays, Munich, 1975,* edited by Klaus Pinkau (Max-Planck-Institut, München, 1975), Vol. 12, p. 4306; Mt. Fuji Collaboration, M. Akashi *et al.*, ICR Report No. 95-81-11, Institute for Cosmic Ray Research, University of Tokyo, 1981 (unpublished).

[4]By scaling in this paper, is meant the (almost) energy-independent inclusive x distribution at $x \gtrsim 0.1$, which we call the fragmentation region. The region of $x < 0.1$ is sometimes called the central region, though it is not the real central region in the center-of-mass system.

[5]P. K. F. Grieder, Rev. Nuovo Cimento 1, 1 (1977).

[6]T. K. Gaisser, R. J. Protheroe, K. E. Turver, and T. J. L. McComb, Rev. Mod. Phys. 50, 859 (1978).

[7]G. B. Khristiansen, in *Sixteenth International Cosmic Ray Conference, Kyoto, 1979, Conference Papers* (Institute of Cosmic Ray Research, University of Tokyo, Tokyo, 1979) Vol. 14, p. 360.

[8]Since most of the particles observed are usually the electromagnetic component, we simply call them γ-ray family. See Ref. 1 for the details of family and experimental conditions of the Mt. Fuji emulsion chamber.

[9]Some authors (Refs. 10,11) use $Z_{ij}=E_iE_j/(E_i+E_j)R_{ij}$ with which we get practically the same result as our case if the characteristic parameter corresponding to χ^c (see text) is set to the half of χ^c.

[10]L. T. Baradzei, Yu. A. Smorodin, and E. A. Solopov, FIAN Report No. 103/104, Moscow, 1974 (unpublished).

[11]C. M. G. Lattes, Y. Fujimoto and S. Hasegawa, Phys. Rep. 65, 1 (1980).

[12]The efficiency of decascading is discussed by A. Tomaszewski and J. A. Wbrotniak, in *Proceedings of the Fourteenth International Conference on Cosmic Rays, Munich, 1975* (Ref. 3), Vol. 7, p. 2361. They show that decascading works well at least for γ rays from one nuclear interaction that occurs at moderate height from the chamber (say, 2—3 radiation lengths) and the interaction energy is not high. We must be aware that decascading does not work for very-high-energy events that occur near the chamber even if only one interaction is involved.

[13]K. Kasahara, S. Torii, and T. Yuda, in *Sixteenth International Cosmic Ray Conference, Kyoto, 1979, Conference Papers* (Ref. 7), Vol. 13, p. 70.

[14]G. Cocconi, Nucl. Phys. 28B, 341 (1971).

[15]Percentage of protons and irons in the total flux (energy/nucleus) is 18% p and 43% Fe at 10^{14} eV, and 11% p and 60% Fe at 10^{15} eV.

[16]We thank the Chacaltaya group for offering us their raw data.

[17]Chacaltaya collaboration, M. Ballester *et al.*, in *17th International Cosmic Ray Conference, Paris, 1981, Conference Papers* (Centre d'Etudes Nucleaires Saclay, 1981), Vol. 11, p. 163.

[18]M. Semba, in *17th International Cosmic Ray Conference, Paris, 1981, Conference Papers* (Ref. 17), Vol. 11, p. 167.

[19]Because the production height is very low and energy is very high decascading with $\chi^c=2$ TeV cm does not work for getting multiplicity at the production point ($N_c=70$ is obtained).

[20]S. Tasaka, *et al.*, ICR Report No. 93-81-9, Institute for Cosmic Ray Research, University of Tokyo, 1981 (unpublished).

[21]Y. Sato, H. Sugimoto, and T. Saito, J. Phys. Soc. Jpn., 41, 1821 (1976).

[22]This cannot be a nucleus-target effect only, because

the authors of Ref. 20 use the same chamber in the accelerator experiment as used in the cosmic-ray case. The authors of Ref. 11 say that new scaling holds at $E_0 > 10$ TeV because their result ($E_0 \sim 100$ TeV) and the balloon experiments at $E_0 \sim 10$ TeV show the same maximum rapidity density. However, we think this is spurious scaling due to the detection loss in the former experiment at $\theta_{\text{lab}} > 2 \times 10^{-4}$, where a considerable number of γ rays have energy less than a few hundred GeV.

[23]To keep the inclusive spectrum at $x > 0.1$ almost constant, there should be collisions which give rise to particles at $x > 0.1$. Such collisions are supposed to have no large heap of particles at $x << 0.1$. The cross sections with and without large heap at $x << 0.1$ should roughly be comparable so that average multiplicity will be of the order of half that of the high-multiplicity events.

[24]Mt. Fuji collaboration, M. Akashi *et al.*, Nouvo Cimento 65A, 355 (1981).

[25]K. Kasahara, in *Proceedings of the Fifteenth International Conference on Cosmic Rays Plovdiv, 1977,* edited by B. Betov (Bulgarian Academy of Sciences, Sofia, 1977), Vol. 7, p. 395.

[26]The relative number of families generated by heavy primaries to those by protons in the original *MSI* model are 0.14 (α) , 0.10 ($M+H$), 0.15 ($VH+$Fe), while by the simple superposition we get corresponding values as 0.13, 0.13, and 0.14.

[27]E. Juliusson, in *Proceedings of the Fourteenth International Conference on Cosmic Rays, Munich, 1975* (Ref. 3), Vol. 8, p. 2689.

[28]V. V. Akimov, N. L. Grigorov, and V. E. Nesterov, *et al,* in *Proceedings of the Eleventh International Conference on Cosmic Rays, Budapest, 1969,* edited by T. Gémesy *et al.* (Akademiai Kiago, Budapest, 1970), Vol. 1, p. 517.

[29]N. L. Grigorov, Yu. V. Gubin, and B. M. Jakovlev, *et al., Proceedings of the Twelfth International Conference on Cosmic Rays, Hobart, 1971,* edited by A. G. Fenton, and K. B. Fenton (University of Tasmania Press, Hobart, Tasmania, 1971), Vol. 1, p. 172.

[30]J. A. Goodman, R. W. Ellsworth, A. S. Ito, *et al.,* Phys. Rev. Lett. 42, 854 (1979); see also R. Cowsik *et al.,* in *17th International Cosmic Ray Conference, Paris, 1981* (Ref. 17), Vol. 2, p. 120.
17), Vol. 2, p. 120.

[31]K. E. Turver, talk in a colloquium at Institute for Cosmic Ray Research, 1981 (unpublished).

[32]Mt. Fuji collaboration, M. Akashi *et al.,* in *Proceedings of the Fifteenth International Conference on Cosmic Rays, Plovdiv, 1977* (Ref. 25), Vol. 7, p. 184; in *Cosmic Rays and Particle Physics—1978,* proceedings at the Bartol Conference, edited by T. K. Gaisser (AIP, New York, 1979), p. 334.

[33]K. Kasahara, S. Torii, and T. Yuda, in *17th International Conference on Cosmic Rays, Paris, 1981* (Ref. 17), Vol. 5, p. 235.